EDGE ARTICLE

Metastable doubly threaded [3]rotaxanes with a large macrocycle†

Jerald E. Hertzog, [ID] [a] Vincent J. Maddi, [ID] [a] Laura F. Hart, [ID] [b] Benjamin W. Rawe, [ID] [b] Phillip M. Rauscher, [ID] [b] Katie M. Herbert, [ID] [bc] Eric P. Bruckner, [ID] [c] Juan J. de Pablo [ID] [bd] and Stuart J. Rowan [ID] *[abcd]

Ring size is a critically important parameter in many interlocked molecules as it directly impacts many of the unique molecular motions that they exhibit. Reported herein are studies using one of the largest macrocycles reported to date to synthesize doubly threaded [3]rotaxanes. A large ditopic 46 atom macrocycle containing two 2,6-bis(*N*-alkyl-benzimidazolyl)pyridine ligands has been used to synthesize several metastable doubly threaded [3]rotaxanes in high yield (65–75% isolated) *via* metal templating. Macrocycle and linear thread components were synthesized and self-assembled upon addition of iron(II) ions to form the doubly threaded pseudo[3]rotaxanes that could be subsequently stoppered using azide−alkyne cycloaddition chemistry. Following demetallation with base, these doubly threaded [3] rotaxanes were fully characterized utilizing a variety of NMR spectroscopy, mass spectrometry, size-exclusion chromatography, and all-atom simulation techniques. Critical to the success of accessing a metastable [3]rotaxane with such a large macrocycle was the nature of the stopper group employed. By varying the size of the stopper group it was possible to access metastable [3]rotaxanes with stabilities in deuterated chloroform ranging from a half-life of <1 minute to *ca.* 6 months at room temperature potentially opening the door to interlocked materials with controllable degradation rates.

Introduction

Even after multiple decades of research, mechanically interlocked molecules (MIMs) continue to inspire chemists and engineers alike on account of their unique interlocked structure and properties.[1–5] Specifically, the synthesis and study of rotaxanes, which are interlocked molecules comprised of dumbbell and ring components, account for over two thirds of all publications involving MIMs.[6,7] This popularity, which is in part a result of their synthetic accessibility, has resulted in their use in a wide range of applications that include molecular machines, catalysis, molecular computing, and drug delivery, to name a few.[8–15] The simplest and most-investigated version of a rotaxane is the singly threaded [2]rotaxane comprised of one macrocycle component kinetically trapped between the large stopper groups of the dumbbell-like component.[16,17] However,

as the field continues to grow, there is increasing interest in looking towards higher order rotaxanes[6,18] (containing more rings, more dumbbells, or both) and their corresponding mechanically interlocked polymers (MIPs).[19,20] This has led to complex architectures capable of advanced function such as molecular elevators,[21,22] artificial molecular muscles,[23,24] molecular pulleys,[25] and more.[9] In addition, polyrotaxane-based materials, such as slide-ring gels,[26,27] have attracted great interest on account of their unique property profiles which have, for example, been commercialized into scratch-resistant coatings.[28] In these materials (and MIPs more broadly), macrocycle size variation has emerged as an important design parameter[19,29–31] with preliminary studies indicating that fluorescence quenching[32] and viscoelastic relaxation dynamics[33] can be tuned by controlling the size of the ring component. As such, there is interest in accessing interlocked polymeric systems with larger rings for further tunability. However, in the literature there appears to be an upper boundary in the size of the macrocycles (around 40 atoms) that are used to synthesize the majority of rotaxane-like structures.

Synthetic efforts targeted at accessing rotaxanes with bigger rings have revealed that even relatively small increases in macrocycle size necessitate dramatic increases in stopper group size.[34,35] Furthermore, investigations into the interlocked stability of rotaxanes have shown that depending on the relative size of the stopper and ring,[36–41] some of these interlocked

[a]Department of Chemistry, University of Chicago, Chicago, IL, 60637, USA. E-mail: stuartrowan@uchicago.edu

[b]Pritzker School of Molecular Engineering, University of Chicago, Chicago, IL 60637, USA

[c]Department of Macromolecular Science and Engineering, Case Western Reserve University, 2100 Adelbert Road, Cleveland, OH 44106, USA

[d]Chemical Science and Engineering Division and Center for Molecular Engineering, Argonne National Laboratory, 9700 S. Cass Ave., Lemont, IL 60434, USA

† Electronic supplementary information (ESI) available. See https://doi.org/10.1039/d2sc01486f

structures are in fact environmentally-dependent metastable rotaxanes,[42] in which the macrocycle is able to slowly slip over the stoppering moiety resulting in the non-interlocked components. Controlling environmental conditions such as temperature, pH, and solvent polarity combined with this unique feature of metastable rotaxanes has been utilized in controlled release applications.[43–45] Furthermore, metastable rotaxanes have been employed in the development of molecular pumps,[46–49] chemical protection,[50–52] modifiable molecular containers,[53] and bacterial imaging probes.[54]

All of the rotaxane materials discussed above are based on singly-threaded architectures. Threading multiple dumbbells within the same macrocyclic cavity offers the unique ability to ensure their close spatial proximity allowing for their physical and optical properties to be influenced.[6] However, doubly threaded [3]rotaxanes have proven extremely challenging from a synthetic standpoint[6] leading to only limited exploration of the corresponding MIPs and higher order rotaxanes.[55–58] As larger macrocycles are typically required to incorporate multiple threads, the difficulty, at least in part, stems from ensuring that the stopper size is large enough to stabilize the interlocked architecture. For example, work by Leigh and coworkers showed that it was possible to access a stable [3]rotaxane with a 38 atom macrocycle, however changing the ring size by just one atom (to 39 atoms) resulted in no isolatable interlocked product.[59] As a result, molecular doubly threaded [3]rotaxanes where both threads exist in a single ring have seen limited high yielding syntheses with reported isolated yields between 6 and 70%.[59–66] In addition, the largest reported macrocycle size used to access such a [3]rotaxane is 41 atoms and the resulting interlocked compound exhibited slow slippage in solution ($t_{1/2} \sim 1$ week at 298 K in dichloromethane).[62] With the goal of accessing multiply threaded higher ordered MIMs and MIPs and developing a better understanding of how to control the stability (and therefore utility) of such structures, reported herein are studies aimed at targeting doubly threaded metastable [3]rotaxanes with a large 46 atom macrocycle.

While a variety of supramolecular templating methods have been utilized to synthesize rotaxanes (such as π–π stacking,[67] hydrogen bonding,[68] hydrophobic interactions,[69] and anion recognition[70]), it is metal ion templating[71–73] (both passive[74–76] and active[77–79]) that has proven to be one of the most popular routes for accessing doubly threaded [3]rotaxanes. While a wide range of ligands have been explored to access mechanically interlocked structures,[72] the terdentate ligand, 2,6-bis(N-alkyl-benzimidazolyl)pyridine (Bip), has a number of attractive features including a flexible and scalable synthesis combined with the ability to tailor its solubility by altering its N-alkyl moieties.[80] It has also been used to access metallosupramolecular assemblies and polymers,[81–85] [2]catenates,[86] [3]catenates,[87] and poly[n]catenanes[88,89] via metal ion coordination. As such, this study utilizes Bip/metal ion templating to access isolatable doubly threaded [3]rotaxanes (Fig. 1a) using one of the largest (46-atom) macrocycles employed to date in rotaxane synthesis and explores how tuning the size of the stoppering group impacts their kinetic stability.
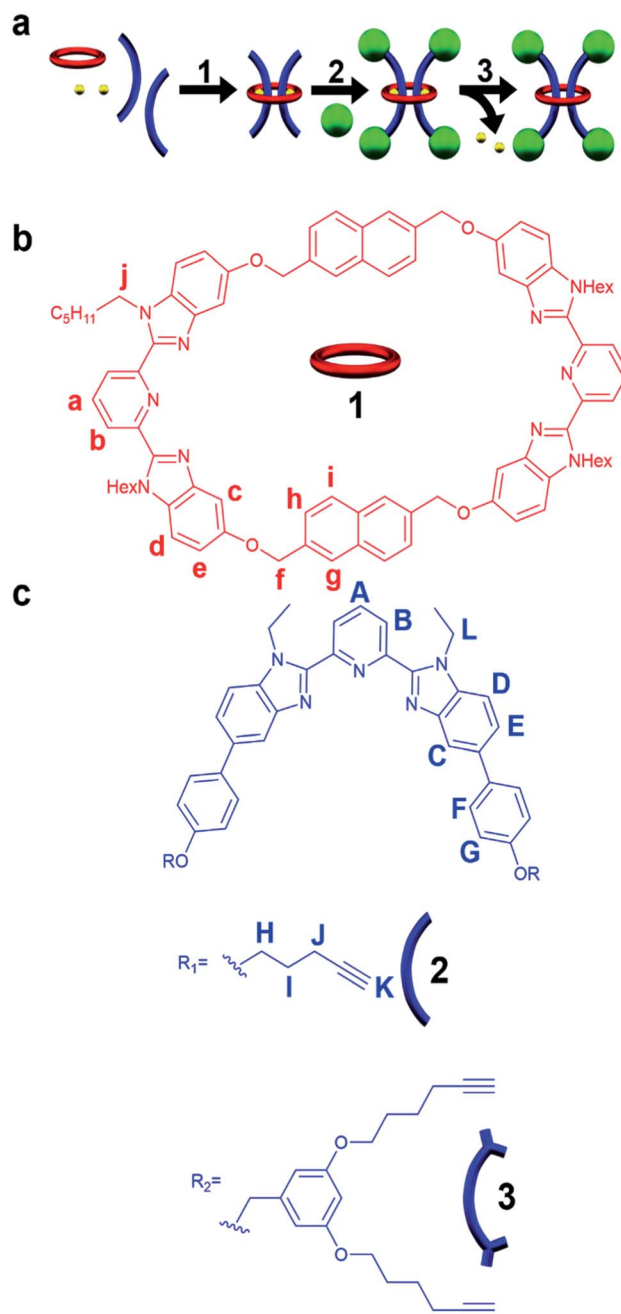

Fig. 1 (a) Cartoon scheme of the doubly threaded [3]rotaxane synthesis that involves metalation of the components with Fe(II) (step 1) followed by addition of the stopper group (step 2) and finally demetallation (step 3). (b) Chemical structure of the 2,6-bis(N-alkyl-benzimidazolyl)pyridine (Bip) containing 46 atom macrocycle 1 and (c) the Bip-containing thread components 2 and 3, ^{1}H NMR assignments indicated.

Results and discussion

Metal-directed self-assembly of the macrocycle with two thread-like components followed by stoppering and demetallation was used to access the [3]rotaxanes (Fig. 1a). The large ditopic Bip-containing macrocycle 1 (Fig. 1b) and the Bip-containing linear thread components 2 and 3 (Fig. 1c) were synthesized

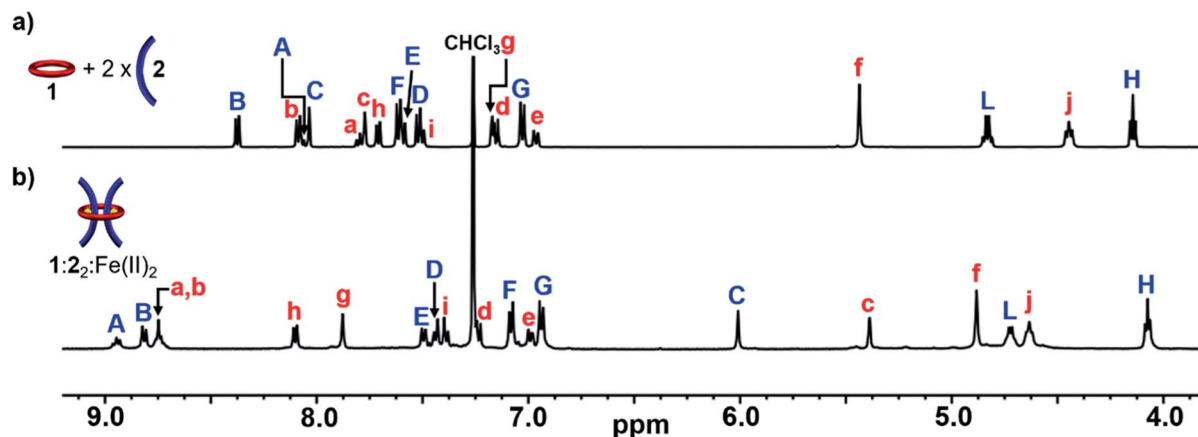**Fig. 2** Partial ^{1}H-NMR spectra of (a) 2 : 1 mixture of **2** : **1** (500 MHz, 25 °C, CDCl$_3$) and (b) **1** : **2**$_2$: Fe(II)$_2$ (500 MHz, 25 °C, 15% d_3-MeCN in CDCl$_3$) after equilibration for 1 day at 45 °C. See Fig. 1 for the corresponding proton assignments.

and fully characterized from their corresponding bis-phenolic Bip derivatives[80,87] *via* Williamson ether synthesis (see ESI, Schemes S1–S6†). **1** is a 46-membered macrocycle incorporating two Bip ligands joined by 2,6-bis(methylene)naphthalene linking units. The rigidity present in the macrocycle was designed to prevent both Bip ligands in **1** binding to the same metal ion and ensure that the only way for these ligands to form 2 : 1 Bip : metal complexes is in the presence of the thread (as confirmed by a UV titration experiment, see ESI, Fig. S1†). The *N*-hexyl substituted Bip ligand in **1** was chosen to aid solubility of the macrocycle, while the thread components **2** and **3** contain an *N*-ethyl substituted Bip ligand to minimize steric repulsion between the thread molecules when both are bound within macrocycle **1**. Components **2** and **3** were end functionalized with terminal alkyne groups (two alkyne moieties in **2** and four alkyne moieties in **3**) in order to allow azide–alkyne cycloaddition[90,91] as the stoppering chemistry.

With **1**, **2** and **3** in hand, and following the synthetic strategy in Fig. 1a, initial studies focused on the self-assembly of the ditopic macrocycle **1** with thread **2** to yield a doubly threaded pseudo[3]rotaxane *via* metal-templating. It is important that the doubly threaded pseudo[3]rotaxane self-assembles efficiently upon metal ion addition for the [3]rotaxane to be formed in high yield. Fe(II) ions have been shown to have a high binding constant with Bip ($>10^{10}$ M^{-2})[92] and were therefore employed as the metal ion templating agent. Initially, a 2 : 1 solution of **2** and **1** in CDCl$_3$ was prepared utilizing ^{1}H-NMR spectroscopy to ensure a 2 : 1 stoichiometry (Fig. 2a).

Upon addition of Fe(NTf$_2$)$_2$ to the 2 : 1 solution an instantaneous color change from colorless to dark purple was observed, indicative of the newly formed Bip-Fe(II) complexes. Monitoring the metalation by ^{1}H-NMR spectroscopy revealed the appearance of new signals corresponding to the metal ion complexed species and a concomitate decrease in the peak intensities that correspond to unbound **1** and **2**. The metal ions were titrated into the sample until no free Bip signals were observed (*ca.* 2 equiv., see ESI, Fig. S2†) and the mixture was equilibrated for 1 day at 45 °C. After equilibration, the ^{1}H-NMR spectrum simplified and, using previously published ^{1}H NMR

spectra of doubly threaded metal-templated Bip complexes,[87–89] it is possible to assign each resonance peak to a given proton in the complex (Fig. 1 and 2b). The obtained doubly threaded pseudo[3]rotaxane is a consequence of the exact stoichiometry employed and the principle of maximal site occupancy.[93] As both ligands in macrocycle **1** are not able to bind to a single metal ion (as confirmed by a UV titration experiment, see ESI,
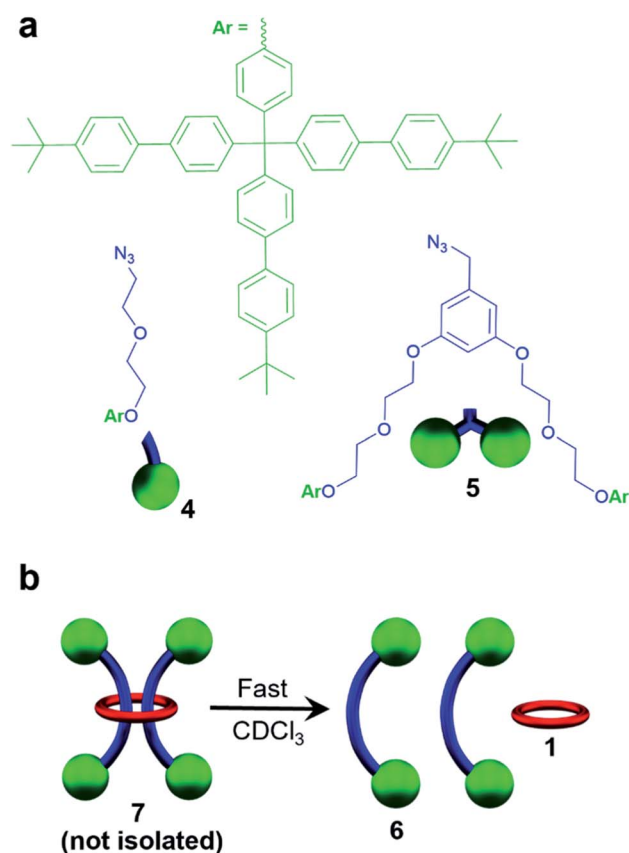

Fig. 3 (a) Chemical structure of stopper groups **4** and **5** used in this study. (b) Cartoon scheme depicting rapid dethreading of **7** seen.
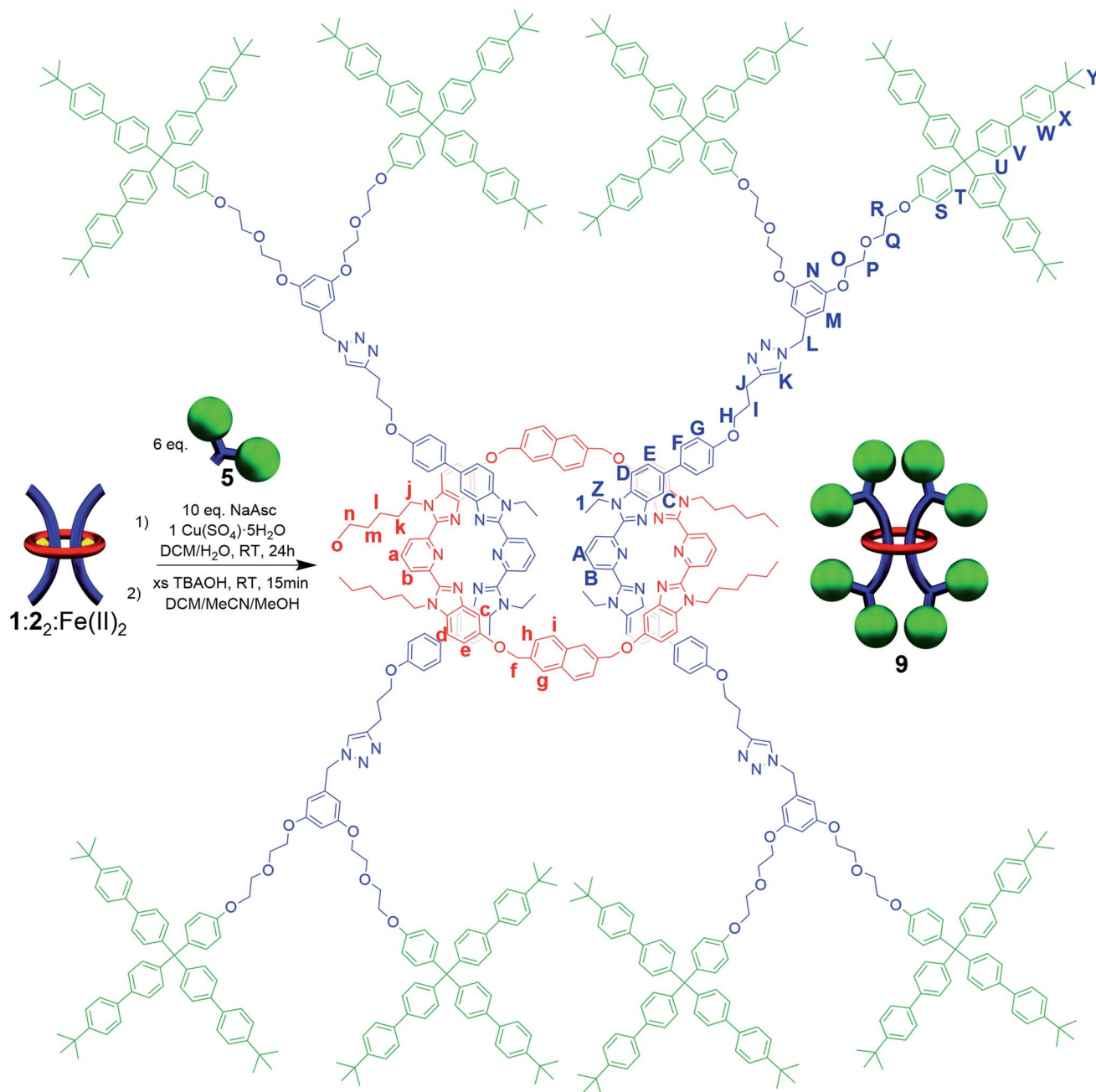
Fig. 4 Scheme showing synthesis and chemical structure of doubly threaded [3]rotaxane 9.

Fig. S1†), the only way for the system to maximize its enthalpic gain, and allow all Bip ligands to form a 2 : 1 Bip : Fe(II) complex, is the formation of the pseudo[3]rotaxane. Comparison of $1 : 2_2 : Fe(II)_2$ to a separately prepared $2_2 : Fe(II)$ assembly confirms no metalated homo thread complexes are present (see ESI, Fig. S3†). Diffusion-ordered spectroscopy (DOSY) (in 15% d_3-MeCN in CDCl$_3$) confirmed the formation of a larger assembly with a diffusion coefficient of 1.6×10^{-10} m^2 s^{-1} compared to 2.9 and 2.3×10^{-10} m^2 s^{-1} for 1 and 2, respectively (see ESI, Fig. S4–7†). These results are consistent with the expected larger hydrodynamic radius of the $1 : 2_2 : Fe(II)_2$ assembly relative to 1 and 2. Similar observations were made

using macrocycle 1 with thread 3 following a similar metalation procedure to form a second doubly threaded pseudo[3]rotaxane $1 : 3_2 : Fe(II)_2$ (for full details, see ESI, Fig. S8–S10 and Scheme S8†).

A macrocycle the size of 1 had not be used to access a [3] rotaxane before, and as such a key goal of this work was to explore different stoppering groups to see what would allow access to isolatable [3]rotaxanes with such a large ring. Initial experiments focused on using the tris(biphenyl)methyl derivative 4 as the stoppering moiety (Fig. 3a) as it is analogous in size to the largest stopper groups used in other reported doubly threaded systems.[64,65] 4 was synthesized with a terminal azide

group (see ESI, Scheme S9–S12† for full synthetic details) in order to react with the alkyne-terminated thread components. In addition, a second stopper group **5** containing two tris(bi-phenyl)methyl moieties was also prepared (Fig. 3a), by reacting a tosyl derivative of the triaryl moieties with the phenolic OH groups in 3,5-dihydroxybenzyl alcohol and subsequently con-verting the benzyl alcohol to a benzyl azide (for full synthetic details see ESI, Schemes S13–S15†). To prepare the [3]rotaxanes, a modified literature procedure[61,62] was employed. **1** : **2**$_2$: Fe(II)$_2$ was stirred in a biphasic (DCM/H$_2$O) mixture of **4** (6 equiv.), Cu(SO$_4$)·5H$_2$O (1 equiv.), and sodium ascorbate (10 equiv.) overnight at room temperature (see ESI, Schemes S16 and S17† for full synthetic details including the synthesis of the free dumbbell **6**). Facile demetallation of the system was achieved using tetrabutylammonium hydroxide as confirmed by a rapid color change of the solution from purple to off-white. The demetallated product was isolated and analysed immediately. Comparison of the crude demetallated ^{1}H-NMR spectrum relative to the starting components confirmed quantitative consumption of the alkyne signal in **2**, and if the ^{1}H NMR spectrum is taken as soon as possible after demetallation (∼4 min), very small signals, upfield from the noninterlocked components, were observed (see ESI, Fig. S11†) that rapidly disappear within a couple of minutes. The presence of such upfield shifted peaks imply these protons are in a more shielded environment, and would be consistent with an interlocked structure.[87–89] A MALDI-TOF MS spectrum (see ESI, Fig. S12†) of the reaction mixture recorded after 6 minutes in solution confirmed only the presence of **1** and **6**, with no signals indic-ative of [3]rotaxane **7**. Any further attempts to optimize the synthesis and isolate **7** were unsuccessful and thus, while the doubly threaded **7** may have been initially formed, these stopper groups are not large enough to prevent the rapid dethreading of the large macrocycle **1** (Fig. 3b) upon demetallation.

While it was not possible to isolate **7**, this result is perhaps not particularly surprising on account of the large size of the ring. As such, efforts turned to exploring [3]rotaxanes featuring the same macrocycle (**1**) and thread (**2**) but with the larger stopper group **5** using the same azide/alkyne cycloaddition conditions and demetallation procedure (Fig. 4) described previously (see ESI, Schemes S18 and S19† for full synthetic details including the synthesis of the free dumbbell **8**).

Similar to what was observed in the crude reaction mixture of the attempted synthesis of **7**, the ^{1}H-NMR analysis of the crude (demetallated) reaction mixture of the targeted synthesis of **9** revealed the presence of new signals that are shifted upfield (on average about 0.15 ppm) from the noninterlocked components. However, this time these upfield signals represent the major product with only a small amount (*ca.* 15%) of noninterlocked byproduct observed (see ESI, Fig. S13†). In addition, no unreacted **2** was detected. Thin layer chromatography (silica, 6% MeOH in CHCl$_3$) confirmed a new single lower R$_f$ product had been formed relative to the noninterlocked components. Preparative thin layer chromatography was then used to sepa-rate the lower R$_f$ product in 75% isolated yield from its non-interlocked byproducts. Utilizing a variety of 1D and 2D NMR techniques (COSY, HSQC, HMBC, see ESI, Fig. S14–S18†)
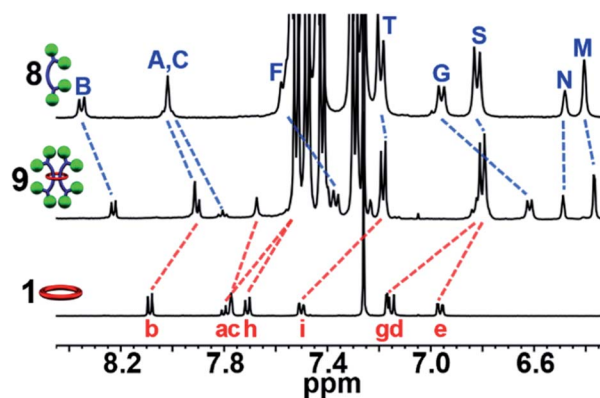

Fig. 5 Partial aromatic ^{1}H-NMR overlay (500 MHz, 25 °C, CDCl$_3$) of **8** (top), **9** (middle), and **1** (bottom), ^{1}H assignments in Fig. 4.
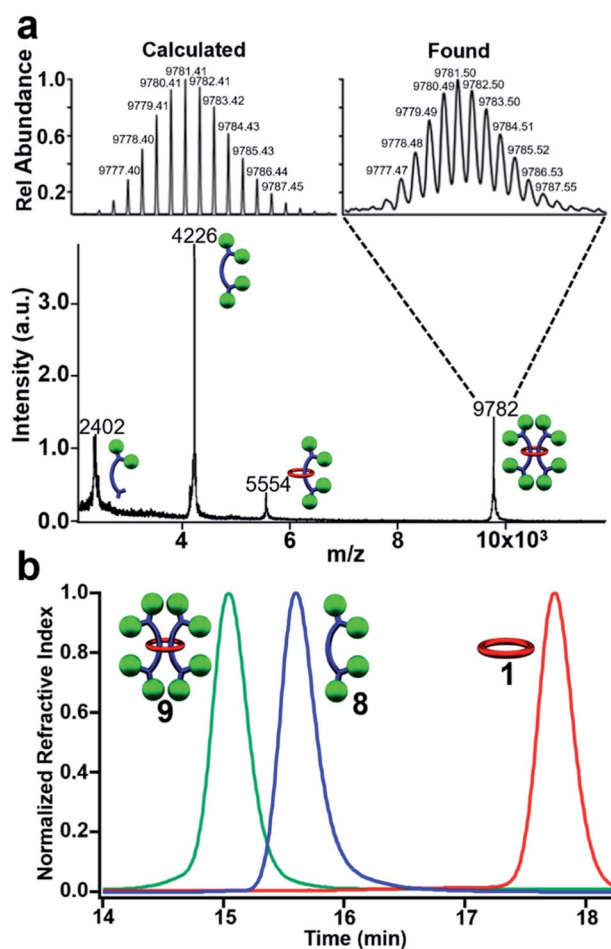

Fig. 6 (a) MALDI-TOF MS of **9** with expansion showing isotopic distribution of the 9782 *m/z* peak (C$_{676}$H$_{696}$N$_{32}$O$_{32}$ (MH$^+$)). (b) GPC chromatogram of (eluent 3 : 1 THF : DMF) of purified **9**, **8**, and **1** at 25 °C.

combined with comparison to the free macrocyclic and dumb-bell components, **1** and **8**, the ^{1}H and ^{13}C{1H}-NMR spectra of **9** could be fully assigned. Fig. 5 shows the diagnostic aromatic region of the ^{1}H NMR (for full spectra see ESI, Fig. S15†).

MALDI-TOF MS of purified **9** (Fig. 6a) shows a high molecular weight peak ((M + H$^+$) m/z: 9782) that is consistent with the targeted [3]rotaxane. Additional lower molecular weight peaks ((M + H$^+$) m/z: 5554, 4226, 2402) are also observed which are consistent with the expected fragmentation pattern of the doubly threaded interlocked structure. Breaking open the macrocycle in **9** results in free dumbbell ((M + H$^+$) m/z: 4226) while fragmentation of a single dumbbell gives the [2]rotaxane ((M + H$^+$) m/z: 5554) and fragmented dumbbell ((M + H$^+$) m/z: 2402) peaks. The high molecular weight peak was further examined using reflectance mode MALDI-TOF to access the mass distribution of **9**. The obtained isotopic distribution displays a clear match to the expected distribution from **9** based on its chemical composition ($C_{676}H_{696}N_{32}O_{32}$ (M + H$^+$)) giving further evidence for the doubly threaded [3]rotaxane **9** (Fig. 6a expansion).

To confirm that **9** was one interlocked molecule free of its noninterlocked components, size exclusion chromatography was employed. GPC analysis using RI detection shows a single peak for **9** with a clear decrease in retention time relative to **8** and **1** (Fig. 6b) as would be expected for the larger doubly threaded architecture. In addition, DOSY NMR was utilized to determine their hydrodynamic radii, which were found to be 1.89, 0.97, and 0.71 nm, for **9**, **8** and **1** respectively (see ESI, Fig. S19–S22†). This roughly doubling in size between **9** and **8** is consistent with the doubly threaded structure.

The close proximity of the interlocked components in **9** was demonstrated using ^{1}H–^{1}H NOESY NMR experiments carried out at 278 K. At this temperature, 10 different intercomponent NOEs could be identified in **9** (Fig. 7a and b) that were not present in a separately prepared 2 : 1 mixture of the dumbbell **8**
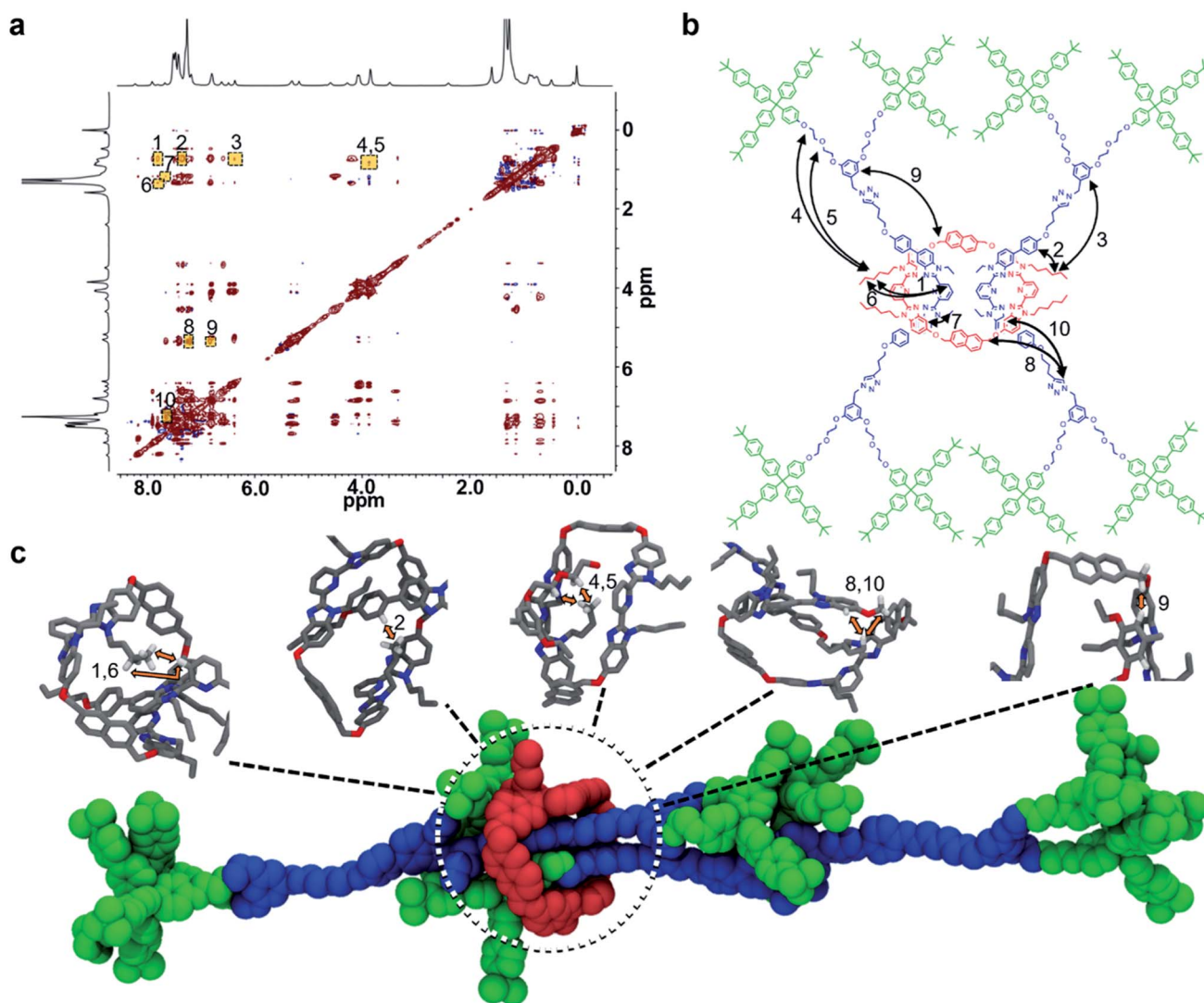

Fig. 7 (a) Full ^{1}H–^{1}H NOESY NMR (500 MHz, CDCl$_3$) of **9** at 278 K. (b) Schematic diagram showing labeled intercomponent NOEs of **9**. (c) All-atom implicit-solvent model renders of **9** showing how NOEs 1, 2, 4, 5, 6, 8, 9, and 10 could arise. In the upper panel, molecular segments are colored according to atom type (gray = carbon, blue = nitrogen, red = oxygen, white = hydrogen). In the bottom panel, the various rotaxane components are colored in accordance with the rest of the figures (red = ring, blue = thread, green = stopper(s)).

and macrocycle **1** at the same concentration (see ESI, Fig. S23–S24†).

NOEs typically arise from distances <5.0 Å (ref. 94) and as such the presence of 10 different intercomponent NOEs confirms that the components of **9** are indeed interlocked. It is interesting to note that there are NOE interactions between **1** and the entire length of the dumbbell component within **9** suggesting that there is some free mobility of the ring along the dumbbell. To better understand how these NOE interactions might occur, all-atom molecular dynamics simulations were conducted to help explore possible rotaxane conformations that could explain the observed NOE signals (Fig. 7c, see ESI and Fig. S25–S29† for full details). The simulations show that the macrocycle typically assumes a position near a stopper group of one dumbbell and in the middle of the other (as shown in Fig. 7c). It is worth pointing out that such conformations are consistent with the majority of the NOEs observed (1, 2, 4, 5, 6, 8, 9, and 10).

During the NMR analysis of **9**, an interesting observation was made. Specifically, after being in solution overnight during ^{13}C {^1H}-NMR acquisition, small trace signals were observed in the ^1H-NMR spectrum that correspond to free dumbbell and macrocycle. As a consequence of this observation and the large size of **1**, it was hypothesized that even with the larger stopper group **5**, very slow slippage may be occurring in solution and that the [3]rotaxane **9** is in fact metastable. As such, the doubly threaded [3]rotaxane **11** (Fig. 8), which effectively doubles the size of the stopper group used in **9**, was targeted. In order to access such a structure, the doubly threaded pseudo[3]rotaxane $1 : 3_2 : Fe(II)_2$ (which contains the thread component **3** with two alkyne moieties on each end group), was stopped with **5** and demetallated using similar conditions to those used to synthesize **9** (see ESI, Schemes S20 and S21† for full synthetic details including the synthesis of the free dumbbell **10**).

^1H-NMR analysis of the crude product again revealed new upfield shifted signals from the noninterlocked components with a small amount (*ca.* 25%) of noninterlocked byproduct observed (macrocycle **1** and dumbbell **10**, see ESI, Fig. S30†) and thin layer chromatography (silica, 5% MeOH in CHCl₃) confirmed a new single lower R_f product had been formed relative to the noninterlocked components. Preparative thin layer chromatography was used to isolate this new product in 65% yield. The entire ^1H NMR spectrum of **11** could be assigned (see ESI, Fig. S31 and S32†) by comparison to the spectra of **1**, **9**,
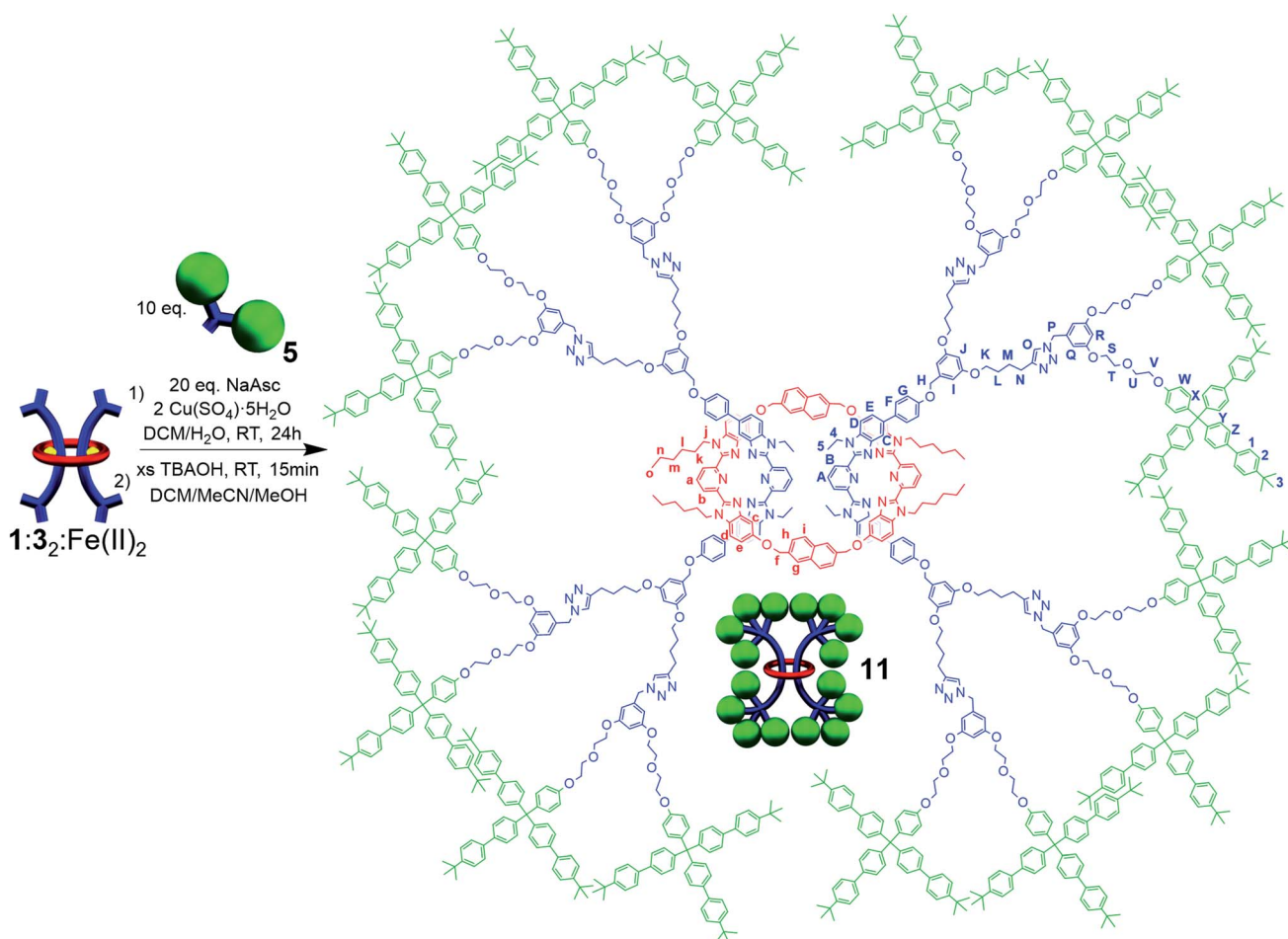

Fig. 8 Scheme showing synthesis and chemical structure of doubly threaded [3]rotaxane **11**.
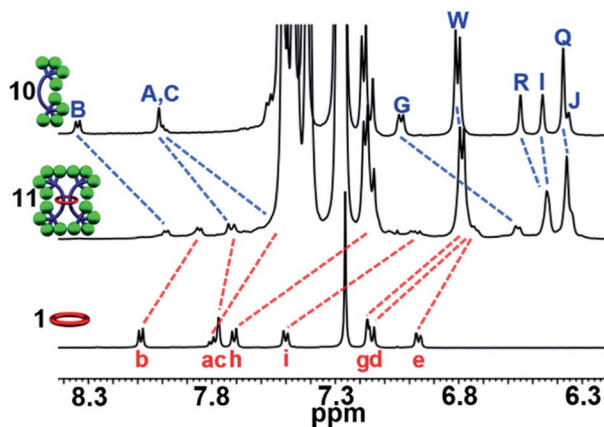
Fig. 9 Partial aromatic ^{1}H-NMR (500 MHz, 25 °C, CDCl$_3$) overlay of **10** (top), **11** (middle), and **1** (bottom), ^{1}H assignments in Scheme S2†.

and **10** combined with ^{1}H–^{1}H COSY of **11** (see ESI, Fig. S33†). Fig. 9 shows the diagnostic aromatic region which reveals an average upfield shift of 0.3 ppm was observed for the aromatic resonances of **11** compared to its noninterlocked components **1** and **10**. It is interesting to note this upfield shift is significantly larger than what was observed for the [3]rotaxane **9**.

GPC analysis using RI detection shows a clear decrease in retention time of **11** relative to its noninterlocked components **10** and **1** (Fig. 10a) and the [3]rotaxane **9** (Fig. 10b) as expected. Finally, MALDI-TOF MS of purified **11** shows the expected fragmentation pattern of the interlocked structure (see ESI, Fig. S34†).
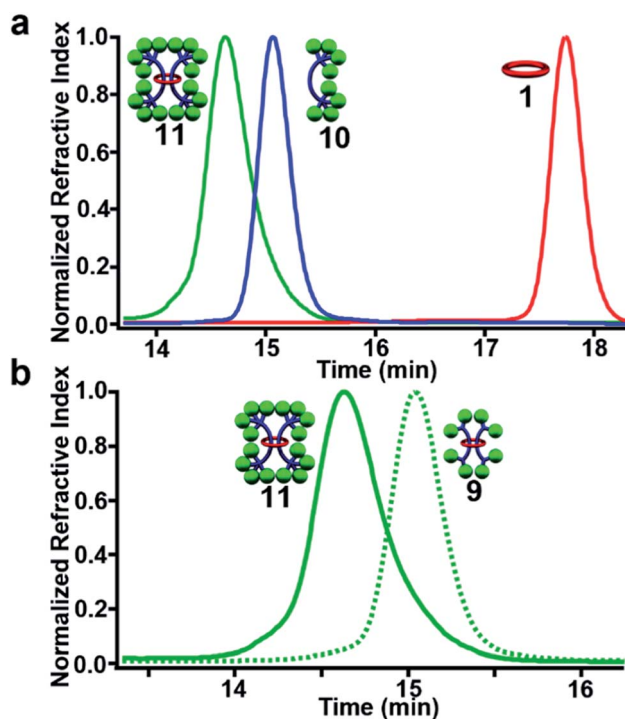

Fig. 10 GPC chromatogram of (3 : 1 THF : DMF as eluent) purified **11**, **10**, and **1** (a) and **11** and **9** (b) at 298 K.

Slippage kinetics of [3]rotaxanes 9 and 11

While the [3]rotaxane **7** was not stable enough to be isolated, both [3]rotaxanes **9** and **11** were isolatable and stable enough to withstand chromatography conditions. None-the-less, as mentioned above the [3]rotaxane **9** appeared to be metastable. Thus, it was decided to explore the lifetime solution stability of both [3]rotaxanes **9** and **11** in more detail. To this end freshly purified solutions of **9** and **11** were monitored *via* ^{1}H NMR spectroscopy at room temperature (25 °C, CDCl$_3$, 1 mM [3] rotaxane) for six weeks. Interestingly in both cases, the upfield shifted protons assigned to the rotaxane slowly decreased in intensity and were replaced with new signals identical to those of the corresponding free dumbbell and macrocycle (see ESI, Fig. S35†) indicative of both compounds undergoing a slow slippage process (Fig. 11a and b). These initial experiments suggested that at 25 °C **9** had a half-life ($t_{1/2}$) of *ca.* 5 weeks while **11** exhibited a $t_{1/2}$ on the order of *ca.* 6 months.

In order to obtain more detailed information on the stability of these metastable double threaded [3]rotaxanes, a full kinetic study was carried out on freshly purified solutions of **9** and **11** in CDCl$_3$ (1 mM [3]rotaxane).[62] Both solutions were monitored at 35 °C for one week followed by 40 °C for another week, and finally 45 °C for a final week with their ^{1}H-NMR spectra recorded at regular time intervals (Fig. 11c and d). This process was repeated in triplicate for both rotaxanes and the concentration of remaining [3]rotaxane in solution could easily be determined from integration of the ^{1}H-NMR spectra at each timepoint (see ESI and Fig. S36–S40† for full details). Standard kinetic analysis revealed the slippage process followed first-order kinetics dependent on the concentration of the [3]rotaxane (*i.e.*, rate of slippage = k_1[rotaxane]) with the indicated half-lives at different temperatures show in Fig. 9e (see ESI, Fig. S41 and S42†). In addition to NMR spectroscopy, GPC was used to confirm that the only new products obtained after the 3 week slippage experiments of **9** and **11** were the corresponding free dumbbell and macrocycle (see ESI, Fig. S43 and S44†). One important observation from both of these studies is that no singly threaded [2]rotaxane intermediate was observed during any of the slippage trials conducted which suggests that any of the corresponding singly threaded [2]rotaxanes using **1** are not stable on any appreciable timescale. This makes sense as it can be expected that the presence of one dumbbell "trapped" within the macrocycle helps to hinder slippage of the second dumbbell.

Standard Arrhenius and Eyring analysis provided the thermodynamic parameters to both slippage processes (Fig. 11e, see ESI, Fig. S45–S48†). Direct comparison to other rotaxane systems in literature is difficult as such data is not typically reported. However, it is worthwhile noting that the activation energy of the slippage process in both **9** (98 ± 4 kJ mol^{-1}) and **11** (112 ± 5 kJ mol^{-1}) are very high compared to the only other doubly threaded [3]rotaxane for which such data is available (35 ± 3 kJ mol^{-1})[62] and is consistent with the very slow slippage process observed in these systems. Comparing **11** to **9** shows that while effectively doubling the number of the tris(*p-t-*
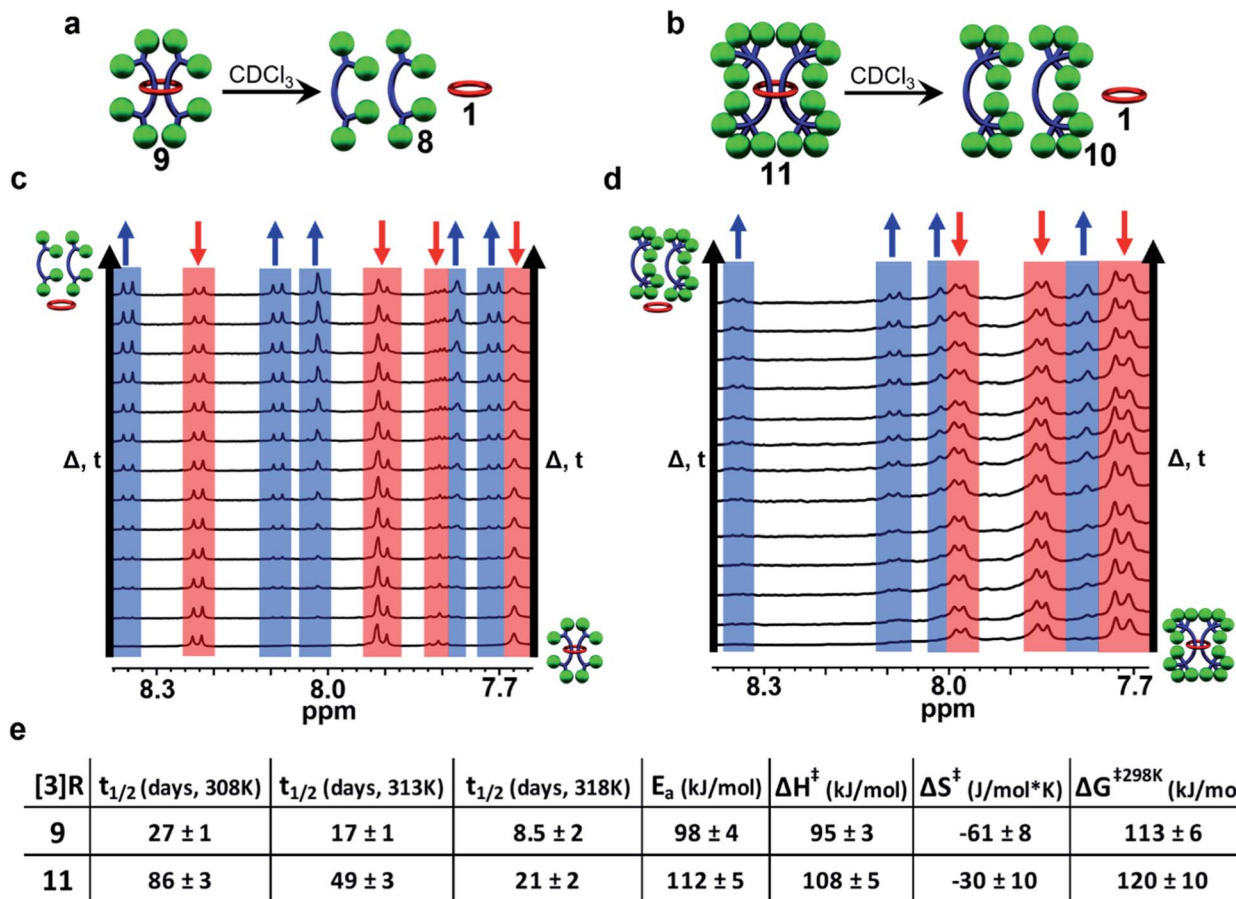
Fig. 11 Scheme illustrating the slippage process of (a) **9** and (b) **11**. Partial ^{1}H-NMR overlay (500 MHz, CDCl$_3$) of a 3 week slippage experiment of (c) **9** and (d) **11**. (e) Table summarizing the kinetic and thermodynamic parameters of the slippage processes of **9** and **11** in CDCl$_3$.

[3]R	$t_{1/2}$ (days, 308K)	$t_{1/2}$ (days, 313K)	$t_{1/2}$ (days, 318K)	E_a (kJ/mol)	$\Delta H^\ddagger$ (kJ/mol)	$\Delta S^\ddagger$ (J/mol*K)	$\Delta G^{\ddagger 298K}$ (kJ/mol)
9	27 ± 1	17 ± 1	8.5 ± 2	98 ± 4	95 ± 3	-61 ± 8	113 ± 6
11	86 ± 3	49 ± 3	21 ± 2	112 ± 5	108 ± 5	-30 ± 10	120 ± 10

butylbiphenyl)methyl moieties on the stopper group does not prevent slippage, it does result in an increase in the energy barrier to dethreading and a dramatic increase in the lifetime stability of the [3]rotaxane ($t_{1/2}$ of 5 weeks *vs.* 6 months at room temperature).

Conclusions

In conclusion, the successful assembly, stoppering, and demetallation of Bip-containing doubly threaded [3]rotaxanes using one of the largest macrocycles reported to date (46 atoms) has been achieved in good yield. On account of the large size of the macrocycle in these interlocked species, all of the [3]rotaxanes synthesized were found to be metastable and that by tuning the number of tris(*p-t*-butylbiphenyl)methyl moieties present in the stoppering unit it was possible to vary their stability with their half-life varying from <1 minute (one tris(*p-t*-butylbiphenyl)methyl moiety) to *ca.* 6 months (four tris(*p-t*-butylbiphenyl)methyl moieties) at room temperature. In fact, two of these metastable [3]rotaxanes were stable enough to withstand column chromatography and allow a full suite of characterization experiments, ^{1}H–^{1}H-NOESY, DOSY, GPC, and MALDI-MS, to confirm their assigned interlocked structure. The extremely slow slippage of [3]rotaxanes **9** and **11** is especially intriguing as

it opens the door to the development of a range of relatively long lived metastable materials. For example, the utilization of such metastable doubly threaded rotaxanes may allow access to polyrotaxane networks/slide ring gels whose degradation rate can be controlled or are able to be reprocessed. Work along these lines is currently underway.

Data availability

The authors declare that all data supporting the findings of this study are available within the article and ESI,† and raw data files are available from the corresponding author upon reasonable request.

Author contributions

Conflicts of interest

There are no conflicts to declare.

Acknowledgements

References

1 J. F. Stoddart, The chemistry of the mechanical bond, *Chem. Soc. Rev.*, 2009, **38**, 1802–1820.

2 C. J. Bruns and J. F. Stoddart, *The Nature of the Mechanical Bond: From Molecules to Machines*, Wiley, 2016, DOI: 10.1002/9781119044123.

3 J.-P. Sauvage, From Chemical Topology to Molecular Machines (Nobel Lecture), *Angew. Chem., Int. Ed.*, 2017, **56**, 11080–11093.

4 B. L. Feringa, The Art of Building Small: From Molecular Switches to Motors (Nobel Lecture), *Angew. Chem., Int. Ed.*, 2017, **56**, 11060–11078.

5 J. F. Stoddart, Mechanically Interlocked Molecules (MIMs)-Molecular Shuttles, Switches, and Machines (Nobel Lecture), *Angew. Chem., Int. Ed.*, 2017, **56**, 11094–11125.

6 P. R. McGonigal, Multiply threaded rotaxanes, *Supramol. Chem.*, 2018, **30**, 782–794.

7 M. Xue, Y. Yang, X. Chi, X. Yan and F. Huang, Development of Pseudorotaxanes and Rotaxanes: From Synthesis to Stimuli-Responsive Motions to Applications, *Chem. Rev.*, 2015, **115**, 7398–7501.

8 S. Erbas-Cakmak, D. A. Leigh, C. T. McTernan and A. L. Nussbaumer, Artificial Molecular Machines, *Chem. Rev.*, 2015, **115**, 10081–10206.

9 H. Y. Zhou, Y. Han and C. F. Chen, PH-controlled motions in mechanically interlocked molecules, *Mater. Chem. Front.*, 2020, **4**, 12–28.

10 D. Dattler, *et al.*, Design of Collective Motions from Synthetic Molecular Switches, Rotors, and Motors, *Chem. Rev.*, 2020, **120**, 310–433.

11 A. Fernandez, *et al.*, Making hybrid [*n*]-rotaxanes as supramolecular arrays of molecular electron spin qubits, *Nat. Commun.*, 2016, **7**, 1–6.

12 J. R. Heath, Wires, switches, and wiring. A route toward a chemically assembled electronic nanocomputer, *Pure Appl. Chem.*, 2000, **72**, 11–20.

13 E. M. G. Jamieson, F. Modicom and S. M. Goldup, Chirality in rotaxanes and catenanes, *Chem. Soc. Rev.*, 2018, **47**, 5266–5311.

14 J. E. M. Lewis, M. Galli and S. M. Goldup, Properties and emerging applications of mechanically interlocked ligands, *Chem. Commun.*, 2017, **53**, 298–312.

15 K. K. Cotí, *et al.*, Mechanised nanoparticles for drug delivery, *Nanoscale*, 2009, **1**, 16–39.

16 I. T. Harrison and S. Harrison, Synthesis of a stable complex of a macrocycle and a threaded chain, *J. Am. Chem. Soc.*, 1967, **89**, 5723–5724.

17 B. Taghavi Shahraki, *et al.*, The flowering of mechanically interlocked molecules: novel approaches to the synthesis of rotaxanes and catenanes, *Coord. Chem. Rev.*, 2020, **423**, 213484.

18 H. Y. Zhou, Q. S. Zong, Y. Han and C. F. Chen, Recent advances in higher order rotaxane architectures, *Chem. Commun.*, 2020, **56**, 9916–9936.

19 L. F. Hart, *et al.*, Material properties and applications of mechanically interlocked polymers, *Nat. Rev. Mater.*, 2021, **6**, 508–530.

20 S. Mena-Hernando and E. M. Pérez, Mechanically interlocked materials. Rotaxanes and catenanes beyond the small molecule, *Chem. Soc. Rev.*, 2019, **48**, 5016–5032.

21 J. D. Bacljić, V. Balzani, A. Credi, S. Silvi and J. F. Stoddart, A Molecular Elevator, *Science*, 2004, **303**, 1845–1849.

22 Y. Yamada, M. Okamoto, K. Furukawa, T. Kato and K. Tanaka, Switchable intermolecular communication in a four-fold rotaxane, *Angew. Chem., Int. Ed.*, 2012, **51**, 709–713.

23 L. Fang, *et al.*, Acid-base actuation of [c2]daisy chains, *J. Am. Chem. Soc.*, 2009, **131**, 7126–7134.

24 G. Du, E. Moulin, N. Jouault, E. Buhler and N. Giuseppone, Muscle-like supramolecular polymers: integrated motion from thousands of molecular machines, *Angew. Chem., Int. Ed.*, 2012, **51**, 12504–12508.

25 Z. Meng and C. F. Chen, A molecular pulley based on a triply interlocked [2]rotaxane, *Chem. Commun.*, 2015, **51**, 8241–8244.

26 Y. Okumura and K. Ito, The polyrotaxane gel: a topological gel by figure-of-eight cross-links, *Adv. Mater.*, 2001, **13**, 485–487.

27 K. Ito, Novel cross-linking concept of polymer network: synthesis, structure, and properties of slide-ring gels with freely movable junctions, *Polym. J.*, 2007, **39**, 489–499.

28 Y. Noda, Y. Hayashi and K. Ito, From topological gels to slide-ring materials, *J. Appl. Polym. Sci.*, 2014, **131**, 40509.

29 P. M. Rauscher, K. S. Schweizer, S. J. Rowan and J. J. de Pablo, Dynamics of poly[*n*]catenane melts, *J. Chem. Phys.*, 2020, **152**, 214901.

30 K. Hagita, T. Murashima and N. Sakata, Mathematical Classification and Rheological Properties of Ring Catenane Structures, *Macromolecules*, 2021, **55**, 166–177.

31 Y. Yasuda, *et al.*, Sliding Dynamics of Ring on Polymer in Rotaxane: A Coarse-Grained Molecular Dynamics Simulation Study, *Macromolecules*, 2019, **52**, 3787–3793.

32 F. E. Oddy, *et al.*, Influence of cyclodextrin size on fluorescence quenching in conjugated polyrotaxanes by methyl viologen in aqueous solution, *J. Mater. Chem.*, 2009, **19**, 2846–2852.

33 K. Kato, K. Karube, N. Nakamura and K. Ito, The effect of ring size on the mechanical relaxation dynamics of polyrotaxane gels, *Polym. Chem.*, 2015, **6**, 2241–2248.

34 S. Saito, K. Nakazono, E. Takahashi and R. V. April, Template Synthesis of [2] Rotaxanes with Large Ring Components and Tris(biphenyl) methyl Group as the Blocking Group. The Relationship between the Ring Size and the Stability of the Rotaxanes, *J. Org. Chem.*, 2006, **71**, 7477–7480.

35 S. Saito, *et al.*, Synthesis of Large [2]Rotaxanes, The Relationship between the Size of the Blocking Group and the Stability of the Rotaxane, *J. Org. Chem.*, 2013, **78**, 3553–3560.

36 F. M. Raymo, K. N. Houk and J. F. Stoddart, The mechanism of the slippage approach to rotaxanes. Origin of the 'all- or-nothing' substituent effect, *J. Am. Chem. Soc.*, 1998, **120**, 9318–9322.

37 A. Affeld, G. M. Hühner, C. Seel and C. A. Schalley, Rotaxane or pseudorotaxane? Effects of small structural variations on the deslipping kinetics of rotaxanes with stopper groups of intermediate size, *Eur. J. Org. Chem.*, 2001, 2877–2890, DOI: 10.1002/1099-0690(200108)2001:15<2877::AID-EJOC2877>3.0.CO;2-R.

38 P. Linnartz, S. Bitter and C. A. Schalley, Deslipping of Ester Rotaxanes: A Cooperative Interplay of Hydrogen Bonding with Rotational Barriers, *Eur. J. Org. Chem.*, 2003, 4819–4829, DOI: 10.1002/ejoc.200300466.

39 C. Heim, A. Affeld, M. Nieger and F. Vögtle, Size complementarity of macrocyclic cavities and stoppers in amide- rotaxanes, *Helv. Chim. Acta*, 1999, **82**, 746–759.

40 J. Groppi, *et al.*, Precision Molecular Threading/Dethreading, *Angew. Chem., Int. Ed.*, 2020, **59**, 14825–14834.

41 M. Händel, M. Plevoets, S. Gestermann and F. Vögtle, Synthesis of Rotaxanes by Brief Melting of Wheel and Axle Components, *Angew. Chem., Int. Ed. Engl.*, 1997, **36**, 1199–1201.

42 P. R. Ashton, *et al.*, Rotaxane or pseudorotaxane? That is the question!, *J. Am. Chem. Soc.*, 1998, **120**, 2297–2307.

43 S. Chiu, *et al.*, A Rotaxane-Like Complex with Controlled-Release Characteristics, *Org. Lett.*, 2000, **2**, 3631–3634.

44 S. Cherraben, J. Scelle, B. Hasenknopf, G. Vives and M. Sollogoub, Precise Rate Control of Pseudorotaxane Dethreading by pH-Responsive Selectively Functionalized Cyclodextrins, *Org. Lett.*, 2021, **23**, 7938–7942.

45 X. Ling, E. L. Samuel, D. L. Patchell and E. Masson, Cucurbituril slippage: Translation is a complex motion, *Org. Lett.*, 2010, **12**, 2730–2733.

46 Y. Qiu, *et al.*, A precise polyrotaxane synthesizer, *Science*, 2020, **368**, 1247–1253.

47 Y. Qiu, *et al.*, A Molecular Dual Pump, *J. Am. Chem. Soc.*, 2019, **141**, 17472–17476.

48 C. Cheng, *et al.*, An artificial molecular pump, *Nat. Nanotechnol.*, 2015, **10**, 547–553.

49 C. Pezzato, *et al.*, An efficient artificial molecular pump, *Tetrahedron*, 2017, **73**, 4849–4857.

50 M. A. Soto, F. Lelj and M. J. MacLachlan, Programming permanent and transient molecular protection: *via* mechanical stoppering, *Chem. Sci.*, 2019, **10**, 10422–10427.

51 M. A. Soto and M. J. Maclachlan, Disabling Molecular Recognition through Reversible Mechanical Stoppering, *Org. Lett.*, 2019, **21**, 1744–1748.

52 S. Y. Hsueh, *et al.*, Protecting a squaraine near-IR dye through its incorporation in a slippage-derived [2]rotaxane, *Org. Lett.*, 2007, **9**, 4523–4526.

53 T. H. Chiang, *et al.*, Using Slippage to Construct a Prototypical Molecular 'lock & Lock' Box, *Org. Lett.*, 2021, **23**, 5787–5792.

54 J. J. Lee, A. G. White, J. M. Baumes and B. D. Smith, Microwave-assisted slipping synthesis of fluorescent squaraine rotaxane probe for bacterial imaging, *Chem. Commun.*, 2010, **46**, 1068–1069.

55 M. M. Fan, Z. J. Yu, H. Y. Luo, S. Zhang and B. J. Li, Supramolecular network based on the self-assembly of γ-cyclodextrin with poly(ethylene glycol) and its shape memory effect, *Macromol. Rapid Commun.*, 2009, **30**, 897–903.

56 K. Iijima, D. Aoki, H. Otsuka and T. Takata, Synthesis of rotaxane cross-linked polymers with supramolecular cross-linkers based on γ-CD and PTHF macromonomers: the effect of the macromonomer structure on the polymer properties, *Polymer*, 2017, **128**, 392–396.

57 K. Yamamoto, R. Nameki, H. Sogawa and T. Takata, Macrocyclic Dinuclear Palladium Complex as a Novel Doubly Threaded [3]Rotaxane Scaffold and Its Application as a Rotaxane Cross-Linker, *Angew. Chem., Int. Ed.*, 2020, **59**, 18023–18028.

58 H. Aramoto, *et al.*, Redox-responsive supramolecular polymeric networks having double-threaded inclusion complexes, *Chem. Sci.*, 2020, **11**, 4322–4331.

59 J. J. Danon, D. A. Leigh, P. R. McGonigal, J. W. Ward and J. Wu, Triply Threaded [4]Rotaxanes, *J. Am. Chem. Soc.*, 2016, **138**, 12643–12647.

60 E. J. F. Klotz, T. D. W. Claridge and H. L. Anderson, Homo- and hetero-[3]rotaxanes with two π-systems clasped in a single macrocycle, *J. Am. Chem. Soc.*, 2006, **128**, 15374–15375.

61 A. I. Prikhod'ko, F. Durola and J. P. Sauvage, Iron(ɪɪ)-templated synthesis of [3]rotaxanes by passing two threads through the same ring, *J. Am. Chem. Soc.*, 2008, **130**, 448–449.

62 A. I. Prikhod'ko and J. P. Sauvage, Passing two strings through the same ring using an octahedral metal center as template: a new synthesis of [3]rotaxanes, *J. Am. Chem. Soc.*, 2009, **131**, 6794–6807.

63 H. M. Cheng, *et al.*, En route to a molecular sheaf: active metal template synthesis of a [3]rotaxane with two axles threaded through one ring, *J. Am. Chem. Soc.*, 2011, **133**, 12298–12303.

64 Y. Yamashita, Y. Mutoh, R. Yamasaki, T. Kasama and S. Saito, Synthesis of [3]rotaxanes that utilize the catalytic activity of a macrocyclic phenanthroline-Cu complex: remarkable effect of the length of the axle precursor, *Chem.–Eur. J.*, 2015, **21**, 2139–2145.

65 R. Hayashi, Y. Mutoh, T. Kasama and S. Saito, Synthesis of [3]Rotaxanes by the Combination of Copper-Mediated Coupling Reaction and Metal-Template Approach, *J. Org. Chem.*, 2015, **80**, 7536–7546.

66 L. D. Movsisyan, *et al.*, Polyyne Rotaxanes: Stabilization by Encapsulation, *J. Am. Chem. Soc.*, 2016, **138**, 1366–1376.

67 M. Asakawa, *et al.*, The slipping approach to self-assembling [*n*]rotaxanes, *J. Am. Chem. Soc.*, 1997, **119**, 302–310.

68 N. H. Evans, Recent Advances in the Synthesis and Application of Hydrogen Bond Templated Rotaxanes and Catenanes, *Eur. J. Org. Chem.*, 2019, 3320–3343, DOI: 10.1002/ejoc.201900081.

69 S. A. Nepogodiev and J. F. Stoddart, Cyclodextrin-based catenanes and rotaxanes, *Chem. Rev.*, 1998, **98**, 1959–1976.

70 J. A. Wisner, P. D. Beer, M. G. B. Drew and M. R. Sambrook, Anion-templated rotaxane formation, *J. Am. Chem. Soc.*, 2002, **124**, 12469–12476.

71 J. E. Beves, B. A. Blight, C. J. Campbell, D. A. Leigh and R. T. McBurney, Strategies and tactics for the metal-directed synthesis of rotaxanes, knots, catenanes, and higher order links, *Angew. Chem., Int. Ed.*, 2011, **50**, 9260–9327.

72 J. E. M. Lewis, P. D. Beer, S. J. Loeb and S. M. Goldup, Metal ions in the synthesis of interlocked molecules and materials, *Chem. Soc. Rev.*, 2017, **46**, 2577–2591.

73 A. Inthasot, S. Te Tung and S. H. Chiu, Using Alkali Metal Ions to Template the Synthesis of Interlocked Molecules, *Acc. Chem. Res.*, 2018, **51**, 1324–1337.

74 J. C. Chambron, *et al.*, Rotaxanes and catenanes built around octahedral transition metals, *Eur. J. Org. Chem.*, 2004, 1627–1638, DOI: 10.1002/ejoc.200300341.

75 J. P. Collin, C. Dietrich-Buchecker, P. Gaviña, M. C. Jimenez-Molero and J. P. Sauvage, Shuttles and muscles: linear molecular machines based on transition metals, *Acc. Chem. Res.*, 2001, **34**, 477–487.

76 J. C. Chambron, V. Heitz and J. P. Sauvage, A rotaxane with two rigidly held porphyrins as stoppers, *J. Chem. Soc., Chem. Commun.*, 1992, 1131–1133, DOI: 10.1039/C39920001131.

77 J. D. Crowley, S. M. Goldup, A. L. Lee, D. A. Leigh and R. T. Mc Burney, Active metal template synthesis of rotaxanes, catenanes and molecular shuttles, *Chem. Soc. Rev.*, 2009, **38**, 1530–1541.

78 M. Denis and S. M. Goldup, The active template approach to interlocked molecules, *Nat. Rev. Chem.*, 2017, **1**, 1–18.

79 J. D. Crowley, K. D. Hänni, A. L. Lee and D. A. Leigh, [2] Rotaxanes through palladium active-template oxidative heck cross-couplings, *J. Am. Chem. Soc.*, 2007, **129**, 12092–12093.

80 B. M. McKenzie, *et al.*, Improved synthesis of functionalized mesogenic 2,6-bisbenzimidazolylpyridine ligands, *Tetrahedron*, 2008, **64**, 8488–8495.

81 M. Burnworth, *et al.*, Optically healable supramolecular polymers, *Nature*, 2011, **472**, 334–337.

82 J. B. Beck, J. M. Ineman and S. J. Rowan, Metal/Ligand-Induced Formation of Metallo-Supramolecular Polymers, *Macromolecules*, 2005, **38**, 5060–5068.

83 M. Kanehara, E. Kodzuk and T. Teranishi, Self-assembly of small gold nanoparticles through interligand interaction, *J. Am. Chem. Soc.*, 2006, **128**, 13084–13094.

84 S. C. Yu, S. Hou and W. K. Chan, Synthesis, metal complex formation, and electronic properties of a novel conjugate polymer with a tridentate 2,6-bis(benzimidazol-2-yl) pyridine ligand, *Macromolecules*, 1999, **32**, 5251–5256.

85 B. T. Michal, B. M. McKenzie, S. E. Felder and S. J. Rowan, Metallo-, thermo-, and photoresponsive shape memory and actuating liquid crystalline elastomers, *Macromolecules*, 2015, **48**, 3239–3246.

86 C. Piguet, G. Bernardinelli, A. F. Williams and B. Bocquet, Formation of the First Isomeric [2]Catenates by Self-Assembly about Two Different Metal Ions, *Angew. Chem., Int. Ed.*, 1995, **34**, 582–584.

87 R. J. Wojtecki, *et al.*, Optimizing the formation of 2,6-bis(*N*-alkyl-benzimidazolyl)pyridine-containing [3]catenates through component design, *Chem. Sci.*, 2013, **4**, 4440–4448.

88 Q. Wu, *et al.*, Poly[*n*]catenanes: Synthesis of molecular interlocked chains, *Science*, 2017, **358**, 1434–1439.

89 M. M. Tranquilli, Q. Wu and S. J. Rowan, Effect of metallosupramolecular polymer concentration on the synthesis of poly[*n*]catenanes, *Chem. Sci.*, 2021, **12**, 8722–8730.

90 M. Meldal and C. W. Tomøe, Cu-catalyzed azide – alkyne cycloaddition, *Chem. Rev.*, 2008, **108**, 2952–3015.

91 K. D. Hänni and D. A. Leigh, The application of CuAAC 'click' chemistry to catenane and rotaxane synthesis, *Chem. Soc. Rev.*, 2010, **39**, 1240–1251.

92 M. Enamullah and W. Linert, Substituent- and solvent-effects on the stability of iron(II)-4-*x*-2,6-bis-(benzimidazol-2′-YL)pyridine complexes showing spin-crossover in solution, *J. Coord. Chem.*, 1996, **40**, 193–201.

93 R. Kramer, J. Lehn, I. Le Bel, U. L. Pasteur and A. Marquis-rigault, Self-recognition in helicate self-assembly: spontaneous formation of helical metal complexes from mixtures of ligands and metal ions, *Proc. Natl. Acad. Sci. U. S. A.*, 1993, **90**, 5394–5398.

94 T. Herrmann, P. Güntert and K. Wüthrich, Protein NMR structure determination with automated NOE-identification in the NOESY spectra using the new software ATNOS, *J. Biomol. NMR*, 2002, **24**, 171–189.